10138 *Inorg. Chem.* **2009**, *48*, 10138–10145
DOI: 10.1021/ic901080r

Inorganic Chemistry
Article

Quantitative Photochemical Formation of $[Ru(tpy)(bpy)H]^+$

Yasuo Matsubara,[†] Hideo Konno,[‡,§] Atsuo Kobayashi,[‡,§] and Osamu Ishitani*[,†]

[†]*Department of Chemistry, Tokyo Institute of Technology, O-okayama 2-12-1, E1-9, Meguro-ku, Tokyo 152-8551, Japan, and* [‡]*Graduate School of Science and Engineering, Saitama University, 255 Shimo-Okubo, Saitama 338-8570, Japan.* [§] *Present address* (*H.K.*)*: Research Institute for Innovation in Sustainable Chemistry, National Institute of Advanced Industrial Science and Technology* (*AIST*)*, 1-1-1 Higashi, Tsukuba 305-8569, Japan;* (*A.K.*) *DIC Corporation, Oaza Komuro, Ina-machi, Kitaadachi-gun, Saitama 362-8577, Japan.*

Received June 4, 2009

Quantitative photochemical production of $[Ru(tpy)(bpy)H]^+$ (Ru-H^+) was achieved by irradiation of $[Ru(tpy)(bpy)(DMF)]^{2+}$ (Ru-DMF^{2+}; DMF = N,N-dimethylformamide) in a tetrahydrofuran (THF) solution containing excess triethylamine (NEt_3). The mechanism of the Ru-H^+ formation was investigated in detail. A photochemical ligand substitution reaction of Ru-DMF^{2+} in THF proceeded to give $[Ru(tpy)(bpy)(THF)]^{2+}$ (Ru-THF^{2+}) with a quantum yield of $(7.6 \pm 0.7) \times 10^{-2}$. In the presence of NEt_3, a similar photochemical ligand substitution reaction also proceeded quickly, but the products were an equilibrium mixture of Ru-THF^{2+} and $[Ru(tpy)(bpy)(NEt_3)]^{2+}$ (Ru-$NEt_3{}^{2+}$) with a considerable amount of Ru-H^+ even in the first stage of the photochemical reaction. The equilibrium constant between Ru-THF^{2+} and Ru-$NEt_3{}^{2+}$ was determined as 6.9 ± 2.1. Irradiation to Ru-$NEt_3{}^{2+}$ gave Ru-H^+ with a quantum yield of $(9.1 \pm 0.5) \times 10^{-3}$. An important intermediate, Ru-$NEt_3{}^{2+}$, was isolated, and its properties were investigated in detail.

Introduction

Construction of photochemical multielectron reduction systems has been one of the most significant barriers to developing artificial photosynthesis that can convert solar energy to chemical energy. Typical examples of this process include photocatalytic hydrogen evolution from water[1] and the reduction of CO_2,[2] which require two (or more) electrons in order to form products such as H_2 and CO. Therefore, a photosensitizer that initiates photochemical single-electron transfer should combine with a catalyst which converts single-electron transfer to a multielectron process. However, such photocatalytic systems initiated by photochemical electron transfer cannot fully reduce organic substrates such as olefins,[3a] carbonyl compounds,[3b] and the coenzyme $NAD(P)^+$,[3c] which require two-electron reduction (i.e., hydrogenation or hydride reduction), since these substrates are also good electron acceptors and radical coupling often competes with the addition of a proton and another electron to the one-electron-reduced species as an intermediate.[4]

There have been only a few photocatalytic systems that mediate only hydride transfer. One such system, a combination of $[Ru(tpy)(bpy)(py)]^{2+}$ (tpy = 2,2′;6′,2″-terpyridine; bpy = 2,2′-bipyridine; py = pyridine) as a photocatalyst and triethylamine (NEt_3) as a reductant, can selectively catalyze the hydride reduction of a $NAD(P)^+$ model compound to the corresponding 1,4-dihydroform.[5] Although this type of photocatalysis is unique because no intermolecular photoelectron transfer process is included in the reaction, both the quantum yield (Φ) and the turnover number (TN) for formation of the 1,4-dihydroform are low ($\Phi < 10^{-8}$, TN $\sim$ 3). We have previously reported that photochemical formation of the hydrido complex $[Ru(tpy)(bpy)H]^+$ should be one of the key processes of photocatalytic hydride transfer,[5] but the detail of this step is still unclear because only 3.5% of $[Ru(tpy)(bpy)H]^+$, based on the starting complex, accumulated in the reaction during steady-state irradiation. Although some intermediates such as a NEt_3-coordinated complex have been proposed, they have not been isolated, and

*To whom correspondence should be addressed. E-mail: ishitani@chem.titech.ac.jp.

(1) (a) Amouyal, E. In *Homogeneous Photocatalysis*; VCH: Weinheim, Germany, 1997; Vol. *2*, pp 263−307. (b) Esswein, A. J.; Nocera, D. G. *Chem. Rev*. **2007**, *107*, 4022–4047.

(2) (a) Arakawa, H..; et al. *Chem. Rev*. **2001**, *101*, 953–996. (b) Fujita, E.; DuBois, D. L. *Carbon Dioxide Fixation*, BNL-67078, Brookhaven National Lab.: Upton, NY, 2000; pp 1−34. (c) Takeda, H.; Koike, K.; Inoue, H.; Ishitani, O. *J. Am. Chem. Soc*. **2008**, *130*, 2023–2031.

(3) (a) Pac, C.; Ihama, M.; Yasuda, M.; Miyauchi, Y.; Sakurai, H. *J. Am. Chem. Soc*. **1981**, *103*, 6495–6497. (b) Ishitani, O.; Yanagida, S.; Takamuku, S.; Pac, C. *J. Org. Chem*. **1987**, *52*, 2790–2796. (c) Pac, C.; Kaseda, S.; Ishii, K.; Yanagida, S.; Ishitani, O. In *Photochemical Processes in Organized Molecular Systems*; North-Holland: Amsterdam, 1991; pp 177−186.

(4) In the case of $NAD(P)^+$ model compounds: (a) Eisner, U.; Kuthan, J. *Chem. Rev*. **1972**, *72*, 1–42. (b) Carelli, V.; Liberatore, F.; Casino, A.; Di Rienzo, B.; Tortorella, S.; Scipione, L. *New J. Chem*. **1996**, *20*, 125–130. (c) Kano, K.; Matsuo, T. *Tetrahedron Lett*. **1975**, 1389–1392.

(5) Ishitani, O.; Inoue, N.; Koike, K.; Ibusuki, T. *J. Chem. Soc., Chem. Commun*. **1994**, 367–368.

 Published on Web 10/07/2009

consequently their properties are not well-understood (eq 1).

$$[Ru(tpy)(bpy)(py)]^{2+} \xrightarrow[NEt_3]{h\nu} [Ru(tpy)(bpy)(NEt_3)]^{2+} \xrightarrow{h\nu} [Ru(tpy)(bpy)H]^{+} \quad (1)$$

Here, we report an improvement of both the efficiency and yield of the photochemical formation of $[Ru(tpy)(bpy)H]^+$ by several orders of magnitude. This optimization relied on detailed mechanistic studies, including the isolation of a critical intermediate.

Experimental Section

General Procedures. ^{1}H NMR spectra were recorded on a JEOL Lambda 400 NMR spectrometer (400 MHz) at 25 °C. UV−vis spectra were recorded using a JASCO V-565 spectrometer or MCPD-2000 (Otsuka Electronic Co.). The reduced products of the $NAD(P)^+$ model compounds were analyzed using a HPLC system with a Nomura ODS-UG-5 column, a Shimazu ST-50 pump, a Shimazu UV-50 detector (wavelength: 320 nm for 1,4-BCF_3H), and a Rheodyne 7125 injector. A mixed solution of $MeOH/KH_2PO_4$−NaOH buffer (0.05 M, 4:1 v/v) was used as the eluent. Electrospray ionization mass spectra were obtained with a Shimazu LCMS-2010A system with HPLC-grade methanol as the mobile phase. Diethylamine was analyzed using a Shimazu GC-17A gas chromatograph and a flame ionization detector (GC-FID) with an InertCap for amines capillary column (GL Sciences Inc.). Wolfram Mathematica 6.0 software was used for global fitting.

Materials. Dimethylformamide (DMF) was dried over 4A molecular sieves and distilled at reduced pressure before use. Tetrahydrofuran (THF) was distilled from Na/benzophenone under a nitrogen atmosphere prior to use. Dichloromethane and triethylamine were dried over calcium hydride and distilled under an argon atmosphere. Dichloromethane-d_2 was dried over calcium hydride, distilled using trap-to-trap techniques, and stored over activated 4A molecular sieves under a nitrogen atmosphere. Other chemicals obtained from commercial sources were used without purification. $RuCl_3 \cdot 3H_2O$ was kindly supplied by Kojima Chemical Co. $NaBAr_4' \cdot 2H_2O$ (Ar′ = 3,5-bis(trifluoromethyl)phenyl) was purchased from ABCR GmbH and Company or prepared by the reported procedure.[6] Anhydrous $NaBAr_4'$ was obtained by the removal of water as the dichloromethane azeotrope prior to use. $[Ru(tpy)(bpy)(py)](PF_6)_2$,[7] $[Ru(tpy)(bpy)H](PF_6)$,[8] $[Ru(tpy)(bpy)Cl](PF_6)$,[9] hexafluorophosphate salts of the 1-benzyl-3-trifluoromethylpyridinium cation (BCF_3^+),[10] and the corresponding 1,4-dihydroforms (BCF_3H)[10] were prepared according to reported methods. $[Ru(tpy)(bpy)Cl](BAr_4')$ was prepared by anion exchange of $[Ru(tpy)(bpy)Cl](PF_6)$ with $NaBAr_4'$ in a dichloromethane solution.

$[Ru(tpy)(bpy)(CF_3SO_3)](BAr_4')$. A dichloromethane solution containing $[Ru(tpy)(bpy)Cl](BAr_4')$ (60.0 mg, 43.2 μmol) and $AgCF_3SO_3$ (11.9 mg, 46.4 μmol) was refluxed for 24 h under an argon atmosphere. The precipitated white solid (AgCl) was removed by filtration. The filtrate was partially evaporated, and then *n*-pentane was added into the solution to afford a brown solid. The solid was collected by filtration and washed with *n*-pentane. Yield: 55.5 mg, 80%. Anal. Calcd for $C_{58}H_{31}BF_{27}N_5O_3SRu$: C, 46.35%; H, 2.08%; N, 4.66%. Found: C, 46.36%; H, 1.78%; N, 4.78%. ESI MS (*m*/*z*): 640.0, $[M]^+$. Calcd: 640.02. ^{1}H NMR data are shown in the Supporting Information.

$[Ru(tpy)(bpy)(DMF)](BAr_4')_2$. A 2 mL DMF solution containing $[Ru(tpy)(bpy)(CF_3SO_3)](BAr_4')$ (46.6 mg, 31.0 μmol) and $NaBAr_4' \cdot 2H_2O$ (29.5 mg, 32.0 μmol) was stirred for 5 min, and then cold water was added. The brown precipitate was collected by filtration, washed with cold water, and dried under a vacuum. The product was dissolved in a minimum amount of diethylether under a nitrogen atmosphere and precipitated a second time by the addition of *n*-pentane. Yield: 63.1 mg, 89%. Anal. Calcd for $C_{92}H_{50}B_2F_{48}N_6ORu$: C, 48.25%; H, 2.20%; N, 3.67%. Found: C, 48.36%; H, 2.12%; N, 3.53%. ESI MS (*m*/*z*): 281.8, $[M]^{2+}$. Calcd: 282.06. UV−vis absorption (DMF and THF) λ_{max}, nm (ε, 10^4 M^{-1} cm^{-1}): 485 (1.0) and 481 (1.0). ^{1}H NMR data are shown in the Supporting Information.

$[Ru(tpy)(bpy)(NEt_3)](BAr_4')_2 \cdot (NEt_3)_{0.4}$.[11] Under a nitrogen atmosphere, $[Ru(tpy)(bpy)(CF_3SO_3)](BAr_4')$ (73.3 mg, 48.8 μmol) was dissolved in CH_2Cl_2 (10 mL), and then $NaBAr_4'$ (43.3 mg, 48.9 μmol) was added to it. The solution was stirred for 30 min, followed by filtration to remove precipitated $NaCF_3SO_3$. To avoid the reaction of the dichloromethane with NEt_3, diethylether (1 mL) was added to the red filtrate, followed by the addition of *n*-pentane to produce a brown precipitate. The precipitate was washed three times with *n*-pentane, dissolved in a minimum amount of diethylether, and then precipitated again by the addition of *n*-pentane. The precipitated solid was washed three times with *n*-pentane and dissolved in a minimum amount of diethylether again. NEt_3 (1 mL) was then added to it, and the solution was evaporated slowly under reduced pressure until a solid began to precipitate. The resulting purple solids were washed with *n*-pentane. Even after the solids were dried under a vacuum for 6 h, ^{1}H NMR spectrum of the dry CD_2Cl_2 solution, which dissolved the solids, indicated that 0.4 equiv of NEt_3 was contained as a solvent of crystallization. Yield: 80.1 mg, 70%. Anal. Calcd for $C_{97.4}H_{64}B_2F_{48}N_{6.4}Ru$: C, 49.60%; H, 2.74%; N, 3.80%. Found: C, 49.21%; H, 3.12%; N, 3.75%. ^{1}H NMR (δ, 396 MHz) spectrum was measured in dry CD_2Cl_2 containing the ruthenium complex (12.1 mM): 9.63 (br, 1H, *bpy*-6), 8.43 (d, 1H, J = 8.1 Hz, *bpy*-3), 8.29 (d, 2H, J = 7.7 Hz, *tpy*-3′), 8.19 (ddd, 1H, J = 8.1, 7.5, 1.5 Hz, *bpy*-4), 8.18 (d, 2H, J = 8.3 Hz, *tpy*-3), 8.09 (d, 1H, J = 8.2 Hz, *bpy*-3′), 7.97 (t, 1H, J = 7.7 Hz, *tpy*-4′), 7.90 (dd, 1H, J = 7.5, 5.8 Hz, *bpy*-5), 7.80 (ddd, 2H, J = 8.3, 7.8, 0.8 Hz, *tpy*-4), 7.72 (m, 16H, BAr_4'-*o*), 7.56 (1H, *bpy*-4′), 7.55 (2H, *tpy*-6), 7.54 (m, 8H, BAr_4'-*p*), 7.22 (dd, 2H, J = 7.8, 6.3 Hz, *tpy*-5), 6.97 (d, 1H, J = 6.0 Hz, *bpy*-6′), 6.83 (ddd, 1H, J = 7.7, 6.0, 1.2 Hz, *bpy*-5′), 2.24 (q, 8.4H, J = 7.2 Hz, $-CH_2-$), 0.78 (t, 12.6H, J = 7.2 Hz, $-CH_3$).

Photochemical Formation of the Hydrido Complex. Under a nitrogen atmosphere, a DMF or THF solution (4 mL) containing $[Ru(tpy)(bpy)(DMF)](BAr_4')_2$ (0.05 mM) and NEt_3 (0 − 4 M) was placed into a quartz cuvette (d = 1 cm) and bubbled with argon for 15 min, and then the cuvette was sealed with a rubber septum (Aldrich Z553921). The sample solution was kept at 25 ± 1 °C using a temperature control unit (TAITEC LabBath LB-21 JR) and irradiated at 436 nm using a 500 W high-pressure Hg lamp (Eikosha Co.) combined with a band-pass filter (436 ± 2 nm, Asahi Spectra Co.). The incident light intensity into the solution was 0.23 ± 0.02 μeinstein s^{-1}, which was determined using a $K_3Fe(C_2O_4)_3$ actinometer.[12] Formation

(6) Reger, D. L.; Wright, T. D.; Little, C. A.; Lamba, J. J. S.; Smith, M. D. *Inorg. Chem.* **2001**, *40*, 3810–3814.
(7) Hecker, C. R.; Fanwick, P. E.; McMillin, D. R. *Inorg. Chem.* **1991**, *30*, 659–666.
(8) Konno, H.; Kobayashi, A.; Sakamoto, K.; Fagalde, F.; Katz, N. E.; Saitoh, H.; Ishitani, O. *Inorg. Chim. Acta* **2000**, *299*, 155–163.
(9) Rasmussen, S. C.; Ronco, S. E.; Mlsna, D. A.; Billadeau, M. A.; Pennington, W. T.; Kolis, J. W.; Petersen, J. D. *Inorg. Chem.* **1995**, *34*, 821–829.
(10) Konno, H.; Sakamoto, K.; Ishitani, O. *Angew. Chem., Int. Ed.* **2000**, *39*, 4061–4063.
(11) (a) Hevia, E.; Perez, J.; Riera, V.; Miguel, D.; Kassel, S.; Rheingold, A. *Inorg. Chem.* **2002**, *41*, 4673–4679. (b) Huhmann-Vincent, J.; Scott, B. L.; Kubas, G. J. *J. Am. Chem. Soc.* **1998**, *120*, 6808–6809.
(12) Kurien, K. C. *J. Chem. Soc. B* **1971**, 2081–2082.

of the hydrido complex $[Ru(tpy)(bpy)H]^+$ (Ru-H^+) was analyzed by three methods as follows: (a) HPLC analysis of BCF_3H formed by the addition of $BCF_3{}^+PF_6{}^-$ (about 0.1 mM) to the irradiated solution, (b) determination using the differential spectrum between, before and after the addition of $BCF_3{}^+$, and (c) ^1H NMR measurement of the irradiated THF-d_8 solution containing Ru-DMF^{2+} (10 mM) and NEt_3 (2 M; Figure S6, Supporting Information). The differential molar extinction coefficient ($\Delta\varepsilon$) at 560 nm was $(9.5 \pm 1.3) \times 10^3\ M^{-1}\,cm^{-1}$ using the reaction of $[Ru(tpy)(bpy)H](PF_6)$ with $BCF_3{}^+PF_6{}^-$. Estimation of the quantum yield is mentioned below. Gas samples were taken using a gastight syringe. The diethylamine was analyzed using GC-FID as described above.

Determination of Equilibrium Constants. $[Ru(tpy)(bpy)(NEt_3)](BAr_4')_2\cdot(NEt_3)_{0.4}$ was dissolved in CD_2Cl_2 (0.55 mL) and transferred to a NMR tube under a nitrogen atmosphere, and then the ^1H NMR spectrum was measured. After the measurement, various volumes of NEt_3 or THF were introduced into the NMR tube, and the ^1H NMR spectrum was recorded again. The behavior of the chemical shift of the methylene and methyl protons in NEt_3 allowed for calculation of the equilibrium constant K_1 between $[Ru(tpy)(bpy)(NEt_3)]^{2+}$ (Ru-$NEt_3{}^{2+}$) and $[Ru(tpy)(bpy)(CD_2Cl_2)]^{2+}$ (Ru-$CD_2Cl_2{}^{2+}$). The concentration of $[Ru(tpy)(bpy)(THF)]^{2+}$ (Ru-THF^{2+}) was directly determined using the proton peaks attributed to the THF ligand.

Results

Photochemical Formation of the Hydrido Complex. In a typical run, a THF solution (4 mL) containing $[Ru(tpy)(bpy)(DMF)]^{2+}$ (Ru-DMF^{2+}; 0.20 μmol) and NEt_3 (2 M) was irradiated using 436 nm monochromatic light for 2 h. The UV−vis absorption spectrum of the irradiated solution (Figure 1a) was quite similar to that of $[Ru(tpy)(bpy)H]^+$ (Ru-H^+),[8] as shown in Figure 1b. After the irradiation, the 1-benzyl-3-trifluoromethylpyridinium cation ($BCF_3{}^+$, 0.5 μmol) was added to the reaction solution as hydride acceptor, giving 0.2 μmol of the corresponding hydride reduction product 1-benzyl-3-trifluoromethyl-1,4-dihydropyridine (1,4-BCF_3H). The differential electronic spectrum of the irradiated solution before and after the addition of $BCF_3{}^+$ (inset in Figure 1a) was almost identical to that obtained by the addition of $BCF_3{}^+$ to a THF solution containing Ru-H^+ and NEt_3 (inset Figure 1b). Comparison between these two differential spectra also indicates that Ru-H^+ was quantitatively formed by the photochemical reaction of Ru-DMF^{2+} with NEt_3.[13] A small amount of water was added to the irradiated solution and then analyzed by GC-FID. A stoichiometric equivalent (with respect to Ru-H^+) of diethylamine, which should be produced via hydrolysis of the two-electron oxidation product of NEt_3, $Et_2N^+{=}CHCH_3$,[14] was formed during the photoreaction. These results clearly indicate that quantitative hydride transfer from NEt_3 to the ruthenium complex proceeds photochemically in THF (eq 2).

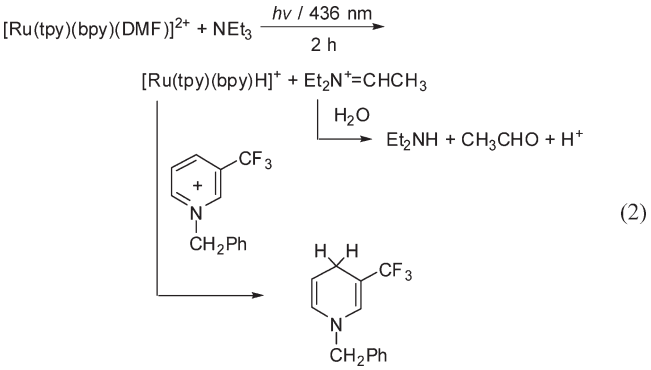

(2)

Figure 2 illustrates the electronic spectral change of the THF solution containing Ru-DMF^{2+} and NEt_3 during irradiation. Although no isosbestic point was observed in the first stage of the photoreaction (0−3 min, shown in Figure 2a), the intensity of the absorption band with a maximum at 485 nm decreased, and new bands appeared at 385 and 544 nm with isosbestic points at 344, 424, and 500 nm after 3 min of irradiation (Figure 2b). The final spectrum obtained by irradiation for 120 min was almost identical to the spectrum of a THF solution containing Ru-H^+ (Figure S1, Supporting Information).

Photochemical Ligand Substitution of Ru-DMF^{2+}. In the absence of NEt_3, irradiation of a THF solution containing Ru-DMF^{2+} caused a rapid blue-shift of the metal-to-ligand charge-transfer absorption band from 481 to 469 nm with isosbestic points at 453 and 393 nm (Figure 3a) within 3 min, which is attributable to photochemical substitution of the DMF ligand with a THF molecule to give $[Ru(tpy)(bpy)(THF)]^{2+}$ (Ru-THF^{2+}, eq 3), but further irradiation did not cause any change of the solution.

$$[Ru(tpy)(bpy)(DMF)]^{2+} \xrightarrow[\text{in THF}]{h\nu} [Ru(tpy)(bpy)(THF)]^{2+} + DMF \quad (3)$$

When the irradiated solution was kept in the dark for 7 h, the UV−vis absorption spectrum of the solution returned to that observed before irradiation (Figure 3b). Because the reformation process of Ru-DMF^{2+} from Ru-THF^{2+} was much slower than the photochemical ligand substitution of Ru-DMF^{2+} with THF and the concentration of THF (12.3 M) was much higher than that of DMF (0.051 mM), irradiation of Ru-DMF^{2+} in THF should cause almost a quantitative conversion to Ru-THF^{2+}. As such, the molar extinction coefficient of Ru-THF^{2+} at 477 nm was estimated as $(9.0 \pm 0.2) \times 10^3\ M^{-1}\,cm^{-1}$. The quantum yield could be determined to be $(7.6 \pm 0.7) \times 10^{-2}$ by fitting the absorption change at 477 nm caused by a growth of peaks attributable to Ru-THF^{2+} and a corresponding decrease of those from Ru-DMF^{2+} ($\varepsilon_{477} = (9.4 \pm 0.2) \times 10^3\ M^{-1}\,cm^{-1}$, Supporting Information).

Synthesis and Identification of $[Ru(tpy)(bpy)(NEt_3)]^{2+}$. The ether complex $[Ru(tpy)(bpy)(OEt_2)]^{2+}$ was chosen as a precursor and was reacted with NEt_3 in a dry diethyl ether solution at room temperature. Evaporation of the

(13) The differential molar extinction coefficient at 560 nm is $(9.5 \pm 1.3) \times 10^3\ M^{-1}\,cm^{-1}$, which was obtained using data shown in the inset in Figure 1b. The ^1H NMR spectrum of a THF-d_8 solution containing Ru-DMF^{2+} and NEt_3 after irradiation also provided clear evidence for the photochemical formation of Ru-H^+, that is, observation of the hydride ligand peak at −14.51 ppm (Figure S6, Supporting Information).

(14) (a) Castedo, L.; Riguera, R.; Vazquez, M. P. *J. Chem. Soc., Chem. Commun.* **1983**, 301–302. (b) Cohen, S. G.; Stein, N. M. *J. Am. Chem. Soc.* **1971**, *93*, 6542–6551. (c) Russell, C. D. *Anal. Chem.* **1963**, *35*, 1291–1292. (d) Smith, P. J.; Mann, C. K. *J. Org. Chem.* **1969**, *34*, 1821–1826.

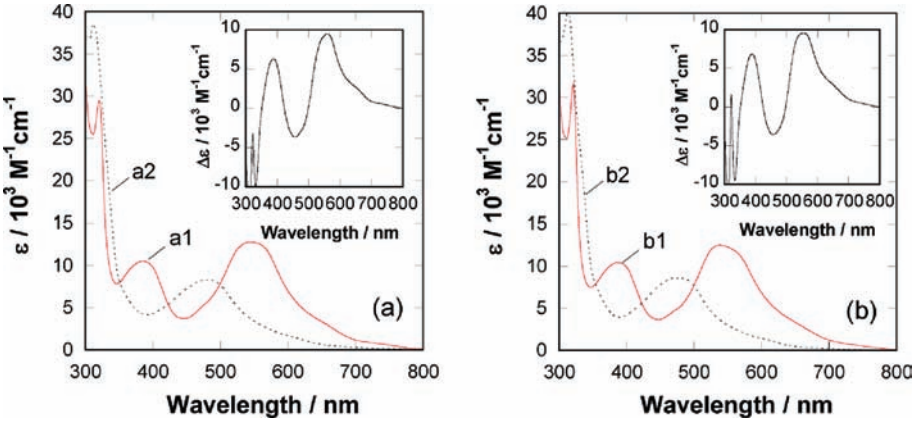

Figure 1. (a) UV−vis absorption spectra of the irradiated THF solutions containing Ru-DMF^{2+} (0.051 mM) and NEt_3 (2 M) for 2 h before (a1) and after (a2) addition of BCF_3^+ (0.125 mM). (b) UV−vis absorption spectra of the THF solution containing Ru-H$^+$ (0.093 mM) and NEt_3 (2 M) before (b1) and after (b2) addition of BCF_3^+ (0.2 mM). Each inset shows differential absorption spectra, that is, a1 − a2 and b1 − b2, respectively.

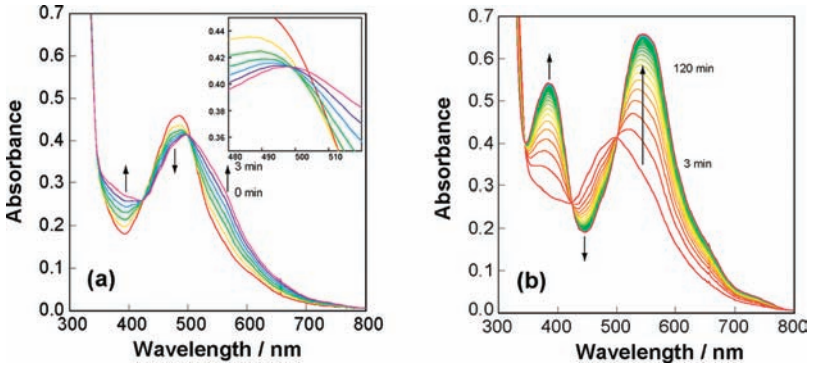

Figure 2. UV−vis absorption spectral changes of a THF solution containing Ru-DMF^{2+} (0.051 mM) and NEt_3 (2 M) during irradiation at 436 nm (a) for 0−3 min recorded at intervals of 0.5 min and (b) for 3−120 min, recorded at intervals of 3 min.

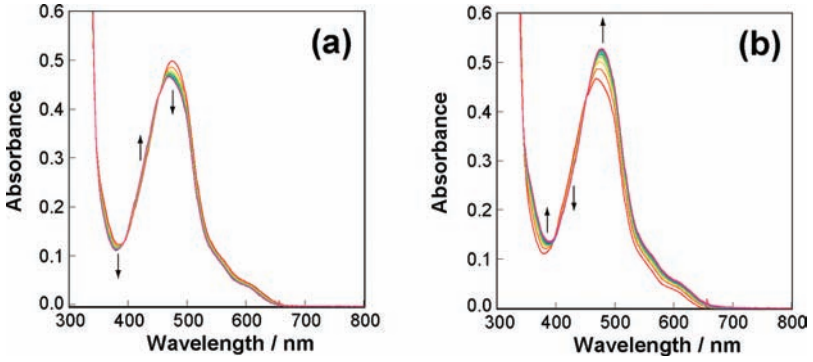

Figure 3. UV−vis absorption spectral changes of a THF solution (4 mL) containing Ru-DMF^{2+} (0.051 mM) during irradiation using 436 nm light (0.23 ± 0.02 μeinstein s^{-1}), recorded up to 3 min at intervals of 10 s (a) and recorded after stopping irradiation at intervals of 30 min (b).

solvent and residual NEt_3, with care taken to exclude moisture, gave a dark red solid [Ru(tpy)(bpy)-(NEt_3)](BAr_4')$_2$ with about half of an equivalent of NEt_3 as the solvent of crystallization, the existence of which was clearly shown by both elemental analysis and ^{1}H NMR. Figure 4 illustrates the ^{1}H NMR spectrum of the Ru-NEt_3^{2+} dissolved in dry CD_2Cl_2. The quartet and triplet peaks attributed to the ethyl groups of the NEt_3 ligand were shifted downfield by 0.23 ppm and 0.20 ppm, respectively, compared with free NEt_3. While the proton peaks at the five and six positions of the bpy ligand were broadened, the other aromatic proton peaks were not.

Equilibrium between Ru-NEt_3^{2+} and Ru-THF^{2+}. Figure 5 shows ^{1}H NMR spectra of a dry CD_2Cl_2 solution containing Ru-NEt_3 (BAr_4)$_2$·0.4NEt_3 (1.8 mM) before and after the addition of NEt_3 (20 mM). It is noteworthy that the concentration of Ru-NEt_3^{2+} in Figure 5a (1.8 mM) was much lower than that in Figure 4 (12.1 mM). Although in all of the cases only one set of proton peaks corresponding to the ethyl groups was observed, their chemical shifts varied depending on the concentrations of NEt_3 and the added complex, as shown in Figure S3 (Supporting Information). These results clearly indicate that there is an equilibrium between Ru-NEt_3^{2+} and

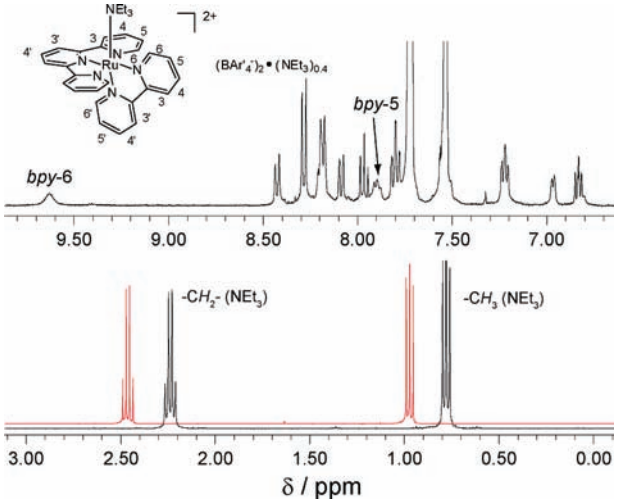

Figure 4. ^{1}H NMR spectra of Ru-NEt_3^{2+} (12.1 mM; black) and free NEt_3 (red) measured in dry CD_2Cl_2 at 25 °C.

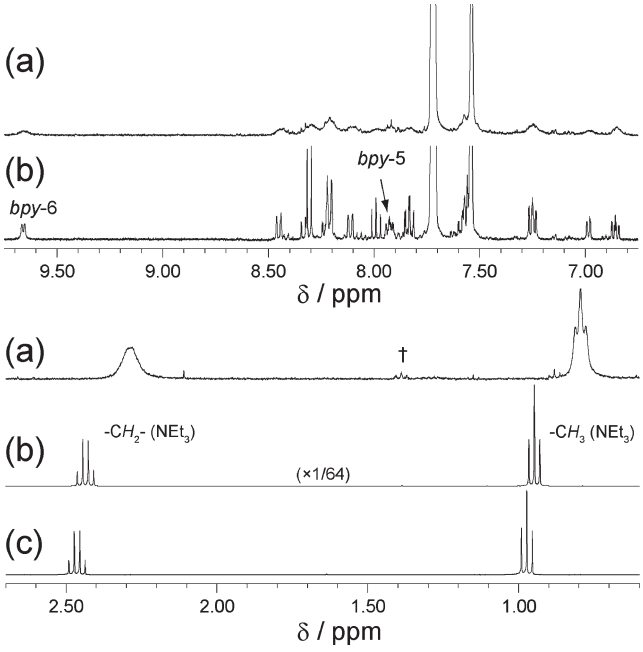

Figure 5. ^{1}H NMR spectra of a CD_2Cl_2 solution containing the Ru-NEt_3^{2+} (1.8 mM) (a) before addition of NEt_3 and (b) after addition of NEt_3 (20 mM). ^{1}H NMR spectrum of CD_2Cl_2 containing only NEt_3 (c). The peak marked with † is attributed to $Et_3N^+-CD_2Cl$, which is produced via a reaction of NEt_3 with CD_2Cl_2 (see ref 15).

a solvent complex, probably $[Ru(tpy)(bpy)(CD_2Cl_2)]^{2+}$ (Ru-$CD_2Cl_2^{2+}$) in this case (eq 4). The equilibrium constant K_1 was obtained as $(9.8 \pm 1.2) \times 10^3$ (Supporting Information).

$$[Ru(tpy)(bpy)(NEt_3)]^{2+} + CD_2Cl_2 \underset{K_1}{\rightleftharpoons} [Ru(tpy)(bpy)(CD_2Cl_2)]^{2+} + NEt_3 \quad (4)$$

The addition of THF to a CD_2Cl_2 solution containing Ru-$NEt_3(BAr_4)_2 \cdot 0.4NEt_3$ affected the ^{1}H NMR chemical shifts attributed to the bpy and tpy ligands and NEt_3 (Figure 6). For example, the ethyl protons were shifted

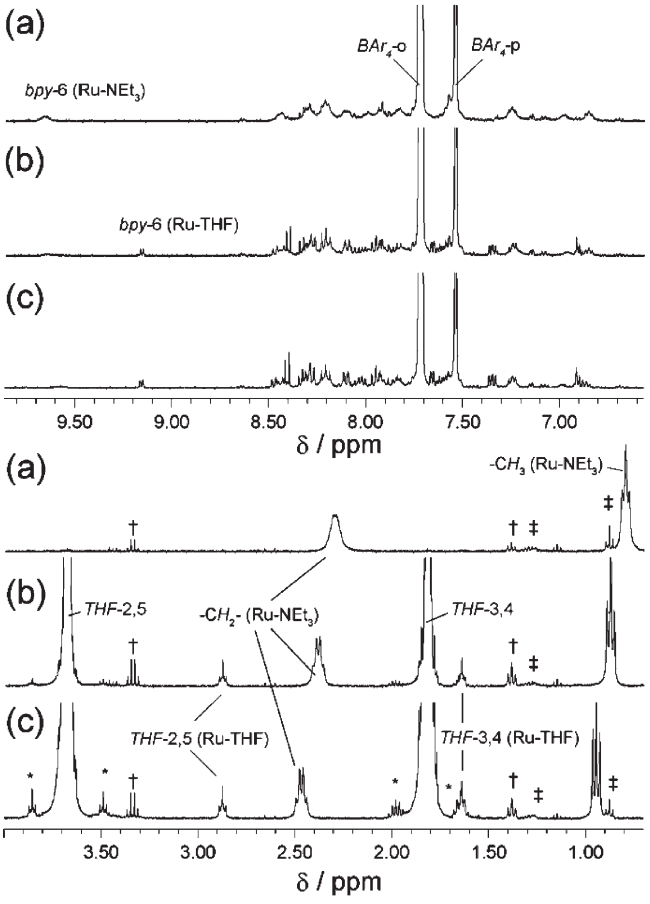

Figure 6. ^{1}H NMR spectra of a CD_2Cl_2 solution containing Ru-NEt_3^{2+} (1.8 mM) before (a) and after the addition of THF (b, 16 mM; c, 30 mM). The peaks marked with ∗ are the spinning side bands. The peaks marked with † are attributed to $Et_3N^+-CD_2Cl$. The peaks marked with ‡ are attributed to contaminating *n*-pentane.

downfield in the presence of a higher concentration of THF. Two sets of protons attributed to THF were observed in the presence of an excess amount of THF, and this ratio did not change even after the sample was kept in the dark for 1 h. The protons attributed to the THF ligand (3.68 and 1.81 ppm) were shifted downfield compared with those of free THF (2.88 and 1.64 ppm). These results indicate that ligand substitution of Ru-NEt_3^{2+} also proceeds with a THF molecule, giving $[Ru(tpy)(bpy)(THF)]^{2+}$ (Ru-THF^{2+}), and that an equilibrium was attained among Ru-NEt_3^{2+}, Ru-THF^{2+}, and Ru-$CD_2Cl_2^{2+}$ as shown in Scheme 1. Calculation of the equilibrium constant K_2 was obtained as $(1.4 \pm 0.4) \times 10^3$ (Supporting Information). Therefore, the equilibrium constant between Ru-NEt_3^{2+} and Ru-THF^{2+} (K) can be determined to be 6.9 ± 2.1 using the relationship $K = K_1/K_2$.

Determination of the Molar Extinction Coefficients of Ru-NEt_3^{2+}. Although the molar extinction coefficient of Ru-NEt_3^{2+} in THF is necessary for determining the true (not apparent) value of the quantum yield of Ru-H^+ formation, it cannot be directly determined using absorption spectra because of its instability. Therefore, we attempted to obtain the quantum yield using the following method. As shown in Figure 2b, the isosbestic points were continuously observed in the electronic spectra of the THF solution containing Ru-DMF^{2+} (0.051 mM)

Scheme 1. Equilibrium among Ru-NEt_3^{2+}, Ru-THF^{2+}, and Ru-$CD_2Cl_2^{2+}$

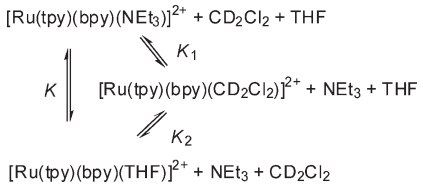

and NEt_3 (2 M) during irradiation with 436 nm light after 3 min of preirradiation. This indicates that three complexes, Ru-THF^{2+}, Ru-NEt_3^{2+}, which are in equilibrium, and the product Ru-H^+, share the irradiated photons during this period (eq 5: $c_{Ru\text{-}H}[t]$ and c_0 are concentrations of Ru-H^+ at time t and the total concentration of the three complexes, respectively, and α is the ratio of Ru-NEt_3^{2+} to the total of Ru-THF^{2+} and Ru-NEt_3^{2+}).

$$\underset{(1-\alpha)(c_0-c_{Ru\text{-}H}[t])}{Ru\text{-}THF^{2+}} \overset{K}{\rightleftharpoons} \underset{\alpha(c_0-c_{Ru\text{-}H}[t])}{Ru\text{-}NEt_3^{2+}} \xrightarrow{h\nu} \underset{c_{Ru\text{-}H}[t]}{Ru\text{-}H^+} \qquad (5)$$

In this case, the absorbance of the reaction solution at 436 nm after irradiation for t sec, measured with a 1 cm cell, is expressed by eq 6 because of the rapid interconversion between Ru-THF^{2+} and Ru-NEt_3^{2+}:

$$\begin{aligned} Abs[t] = &\{\varepsilon_{Ru\text{-}THF}(1-\alpha) \\ &+ \varepsilon_{Ru\text{-}NEt3}\alpha\}(c_0 - c_{Ru\text{-}H}[t]) \\ &+ \varepsilon_{Ru\text{-}H}c_{Ru\text{-}H}[t] \end{aligned} \qquad (6)$$

where $\varepsilon_{Ru\text{-}THF}$ and $\varepsilon_{Ru\text{-}NEt3}$ denote the molar absorption coefficients of Ru-THF^{2+} and Ru-NEt_3^{2+}, respectively. The molar extinction coefficient of Ru-H^+ ($\varepsilon_{Ru\text{-}H}$) is (4.0 $\pm$ 0.1) $\times$ 10^3 M^{-1} cm^{-1}, and $c_{Ru\text{-}H}$ and $\varepsilon_{Ru\text{-}THF}$ (ε = (6.5 $\pm$ 0.2) $\times$ 10^3 M^{-1} cm^{-1}) could be obtained by the procedures described above. The best-fit curve shown in Figure 7 was obtained using eq 6 with $\varepsilon_{Ru\text{-}NEt3}$ = (4.4 $\pm$ 0.5) $\times$ 10^3 M^{-1} cm^{-1} and α = 0.11, 0.20, 0.34, 0.46, and 0.54 for each concentration of NEt_3 (0.5, 1, 2, 3, and 4 M), respectively. We can also estimate the equilibrium constant between Ru-THF^{2+} and Ru-NEt_3^{2+} to be K = 3.8 $\pm$ 1.5 by this method. This value is reasonably consistent with that obtained using NMR techniques (6.9 $\pm$ 2.1).

Determination of Quantum Yields. As described above, Ru-H^+ was produced quantitatively from the equilibrium mixture of Ru-THF^{2+} and Ru-NEt_3^{2+}. Because interconversion between Ru-THF^{2+} and Ru-NEt_3^{2+} is rapid enough to reach equilibrium during irradiation, the molar absorption coefficient of the equilibrium mixture ε_{eq} can be defined by eq 7:

$$\varepsilon_{Ru\text{-}THF}c_{Ru\text{-}THF}[t] + \varepsilon_{Ru\text{-}NEt3}c_{RuNEt3} = \varepsilon_{eq}c_{eq}[t] \qquad (7)$$

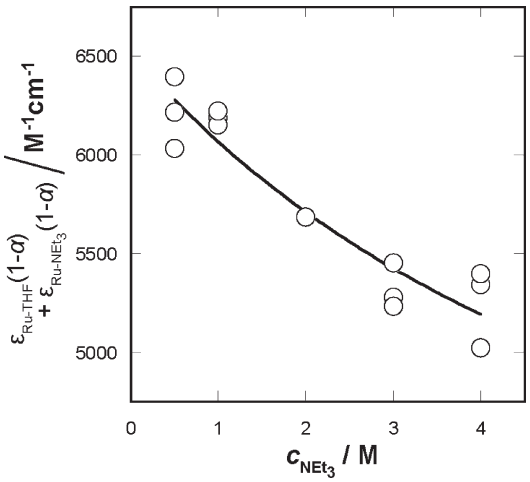

Figure 7. Total absorbance attributed to Ru-THF^{2+} and Ru-NEt_3^{2+} at 436 nm in the presence of various concentrations of NEt_3. The curve was fit using eq 6.

where $c_{Ru\text{-}THF}[t]$, $c_{Ru\text{-}NEt3}[t]$, and $c_{eq}[t]$ denote the concentrations of Ru-THF^{2+} and Ru-NEt_3^{2+} and their total concentration ($c_{Ru\text{-}THF}[t]$ + $c_{Ru\text{-}NEt3}[t]$), respectively, at time t. Because the reaction solution was well-stirred during irradiation, the concentration of each complex should be homogeneous. Therefore, the rate of formation of Ru-H^+ is described by eq 8:[16]

$$\begin{aligned} \frac{dc_{Ru\text{-}H}[t]}{dt} = &\Phi_{app}\frac{I_0}{V}\left\{1-10^{-(\varepsilon_{eq}c_{eq}[t]+\varepsilon_{Ru\text{-}H}c_{Ru\text{-}H}[t])}\right\} \\ &\times \frac{\varepsilon_{eq}c_{eq}[t]}{\varepsilon_{eq}c_{eq}[t] + \varepsilon_{Ru\text{-}H}c_{Ru\text{-}H}[t]} \end{aligned} \qquad (8)$$

where Φ_{app} is the apparent quantum yield of the formation of Ru-H^+ from the equilibrium mixture. I_0 represents photon flux, V is the volume of the solution, and the light-path length of the cuvette was 1 cm. The term in the curly brackets represents the ratio of light absorbed by all of the complexes to the total light flux, and the last term represents the ratio of light absorbed by Ru-THF^{2+} and Ru-NEt_3^{2+} to that by all of the complexes in the solution. The global-fitting method for determining Φ_{app} using eqs 6 and 8 was applied to the absorption change during irradiation between 350 and 650 nm. As an example, Figure 8 shows the absorption changes at 436 and 550 nm during irradiation and the best-fit curves in the case, where a THF solution containing Ru-DMF^{2+} (0.051 mM) and NEt_3 (2 M) was used. Using this fit, the apparent quantum yield of the Ru-H^+ formation (Φ_{app}) was (3.4 $\pm$ 0.2) $\times$ 10^{-3}. The apparent quantum yield Φ_{app} was strongly dependent on the concentration of NEt_3, as shown in Figure S5 (Supporting Information).

Discussion

Irradiation of a THF solution containing Ru-DMF^{2+} and an excess of NEt_3 quantitatively produced Ru-H^+ and NEt_2H as the two-electron oxidation product of NEt_3 (eq 2). Figure 9 shows a dependence of the yield of Ru-H^+ on the irradiation time in photochemical reactions with NEt_3

(15) The chloride complex $[Ru(tpy)(bpy)Cl]^+$ formed by the slow reaction of Ru-$CD_2Cl_2^{2+}$ with NEt_3 accompanied by the formation of Et_3N^+-CD_2Cl (see: Wulff, C. A.; Wright, D. A. *J. Org. Chem.* **1970**, *35*, 4252 and Huhmann-Vincent, J.; Scott, B. L.; Kubas, G. J. *Inorg. Chem.* **1999**, *38*, 115). This reaction was slowed drastically in the presence of NEt_3, THF, or both additives. Therefore, for the calculation of the equilibrium constants, the amount of $[Ru(tpy)(bpy)Cl]^+$ produced just before the addition of NEt_3 and THF was subtracted from the total amount of the added complex. The ^{13}C NMR technique is not suitable for determining the structure of the Ru-$CD_2Cl_2^{2+}$ because of too rapid an exchange between CD_2Cl_2 and NEt_3 as a ligand.

(16) (a) Bunce, N. J. *J. Photochemistry* **1987**, *38*, 99–108. (b) Tonne, J.; Prinzbach, H.; Michl, J. *J. Photochem. Photobiol. Sci.* **2002**, *1*, 105–110.

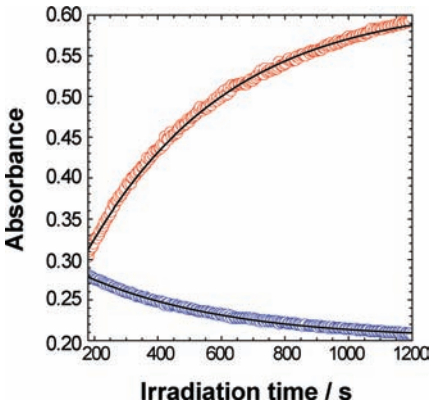

Figure 8. UV−vis absorption changes of a THF solution containing Ru-DMF^{2+} (0.051 mM) and NEt_3 (2 M) during irradiation with 436 nm light for 180−1200 s recorded with 5 s intervals, detected at 436 nm (blue circle) and 550 nm (red circle). The fitting curves were obtained using eqs 6 and 8.

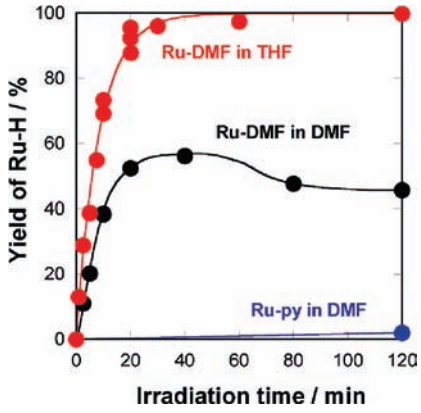

Figure 9. Formation yield of the Ru-H^+ versus irradiation time for the photochemical reactions of Ru-DMF^{2+} in THF (red), Ru-DMF^{2+} in DMF (black), and Ru-py^{2+} in DMF (blue). The solutions containing the complex (0.05 mM) and NEt_3 (2.0 M) were irradiated using 436 nm light (0.23 ± 0.02 μeinstein s^{-1}) under an Ar atmosphere.

(2 M) under three different conditions: using Ru-DMF^{2+} in a THF solution, Ru-DMF^{2+} in DMF, and $[Ru(tpy)(bpy)(py)]^{2+}$ (Ru-py^{2+}) in DMF. This indicates that the photochemical formation of Ru-H^+ is strongly dependent on both the monodentate ligand in the starting complex as well as the solvent. It should be noted that the apparent quantum yield of Ru-H^+ formation using Ru-DMF^{2+} in THF increased by about 5 orders of magnitude over that using Ru-py^{2+} in DMF,[5] which are similar conditions to those reported previously. The formation yield of Ru-H^+ was also improved from 3.5% (Ru-py^{2+} in DMF) to 100% (Ru-DMF^{2+} in THF), depending on the Ru complex added. One of the reasons for this drastic improvement should be the high efficiency and chemoselectivity of the photochemical ligand substitution reaction of Ru-DMF^{2+} ($\Phi = (7.6 \pm 0.7) \times 10^{-2}$ in eq 3). Although similar photochemical ligand substitution of Ru-py^{2+} was observed, its quantum yield was much lower ($\Phi < 10^{-5}$), and no isosbestic point was observed in the spectral change during irradiation.

Although the triethylamine complex Ru-$NEt_3{}^{2+}$ should be an important intermediate in the photochemical formation of Ru-H^+, it had not been isolated because of its instability. Therefore, its properties and reactivity had not been previously studied. We successfully synthesized and isolated Ru-$NEt_3{}^{2+}$ as a $BAr_4'^-$ salt (Ar′ = 3,5-bis(trifluoromethyl)phenyl). As shown in Figure 4, there are no peaks corresponding to free NEt_3 in the ^1H NMR spectrum of Ru-$NEt_3{}^{2+}$. This strongly suggests that the NEt_3 ligand in Ru-$NEt_3{}^{2+}$ is quickly exchanged with free NEt_3, with a pedigree as a solvent of crystallization, on the NMR time scale. The chemical shift and shape of the ^1H NMR peaks were strongly dependent on the concentrations of both Ru-$NEt_3{}^{2+}$ and NEt_3: (1) A lower concentration of the complex without the addition of NEt_3, where the concentration of free NEt_3 should also be low, caused broader peaks of the NEt_3 and the bpy and tpy ligands (Figure 4 and 5a). (2) The addition of NEt_3 caused peak sharpening, and both the ethylene and methylene protons shifted downfield (Figure 5b). These results also indicate a quick exchange of the NEt_3 ligand with free NEt_3 in solution. The equilibrium constant (K_1 in eq 4) between Ru-$NEt_3{}^{2+}$ and the solvento complex $[Ru(tpy)(bpy)(CD_2Cl_2)]^{2+}$ (Ru-$CD_2Cl_2{}^{2+}$) was calculated to be $(9.8 \pm 1.2) \times 10^3$ by use of the dependence of chemical shifts of the ethyl protons on the concentration of NEt_3 in a CD_2Cl_2 solution (Figure S3, Supporting Information). Two pairs of proton peaks attributable to THF were observed through the addition of THF to a CD_2Cl_2 solution containing Ru-$NEt_3{}^{2+}$ (1.8 mM), as shown in Figure 6. The concentration of THF affected the chemical shifts of proton peaks corresponding to NEt_3. This indicates that Ru-$NEt_3{}^{2+}$, Ru-$CD_2Cl_2{}^{2+}$, and Ru-THF^{2+} are in equilibrium with each other in solution. The equilibrium constant between Ru-$NEt_3{}^{2+}$ and Ru-THF^{2+} (K) was calculated as 6.9 ± 2.1.

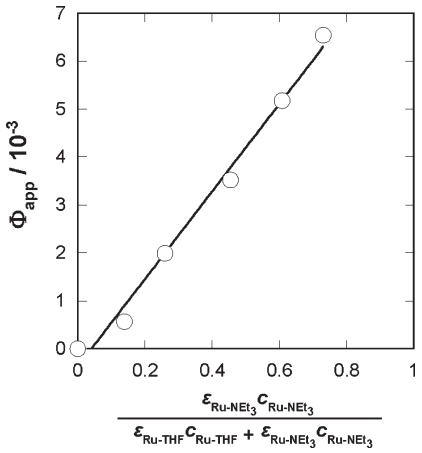

Figure 10. Dependence of the quantum yield of the formation of Ru-H^+ on the ratio of photons absorbed by Ru-$NEt_3{}^{2+}$ to that by the equilibrium mixture of Ru-THF^{2+} and Ru-$NEt_3{}^{2+}$ at 436 nm.

With this data in hand, we can consider the reaction mechanism of the photochemical formation of Ru-H^+. Irradiation of Ru-DMF^{2+} in a THF solution containing NEt_3 leads to a loss of the DMF ligand and a coordination of THF or NEt_3 to give Ru-THF^{2+} and Ru-$NEt_3{}^{2+}$ in a ratio that is dependent on the concentration of NEt_3 in the solution (Scheme 2).

Because the photochemical ligand substitution was completed in the fast stage of the photochemical reaction (within 3 min of irradiation with a light intensity of 0.23 ± 0.02 μeinstein s^{-1}), this process should not affect the efficiency of the following process. The ratio of Ru-THF^{2+} to Ru-$NEt_3{}^{2+}$ in solution is about 4:6 in the presence of 2 M NEt_3. Irradiation of Ru-$NEt_3{}^{2+}$ in the solution containing NEt_3

Scheme 2. Photochemical Ligand Substitution of Ru-DMF^{2+} in THF Containing NEt_3

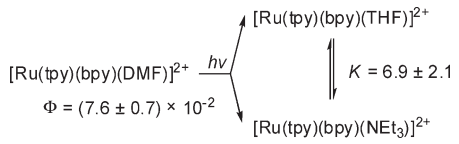

(2 M) caused the formation of Ru-H^+ with an apparent quantum yield (Φ_{app}) of $(3.4 \pm 0.2) \times 10^{-3}$. The apparent quantum yield was strongly dependent on the concentration of NEt_3, as shown in Figure S5 (Supporting Information). It has been previously reported that the irradiation of Ru-NEt_3^{2+} causes the formation of Ru-H^+.[5] An intermolecular photochemical reaction of Ru-THF^{2+} with free NEt_3 might be omitted because of the short lifetime of the excited state of Ru-THF^{2+}, which does not emit at room temperature in THF solution. Therefore, if the formation of Ru-H^+ is caused only by irradiation to Ru-NEt_3^{2+}, the true (not apparent) value of the quantum yield for the photochemical formation of Ru-H^+ from Ru-NEt_3^{2+} ($\Phi_{Ru\text{-}H}$) can be calculated as about $(9.1 \pm 0.5) \times 10^{-3}$ using eq 9, with an equilibrium constant $K = 6.9 \pm 2.1$ and the molar extinction coefficients of the complexes at the irradiation wavelength, that is, 436 nm ($\varepsilon_{Ru\text{-}THF} = (6.5 \pm 0.2) \times 10^3$ M^{-1} cm^{-1} for Ru-THF^{2+} and $\varepsilon_{Ru\text{-}NEt3} = (4.2 \pm 0.9) \times 10^3$ M^{-1} cm^{-1} for Ru-NEt_3^{2+}). A good linear relationship (Figure 10) also strongly supports the hypothesis that the formation of Ru-H^+ occurs via the excitation of Ru-NEt_3^{2+} but not Ru-THF^{2+}.

$$\Phi_{app} = \frac{\varepsilon_{Ru\text{-}NEt3} c_{Ru\text{-}NEt3}}{\varepsilon_{Ru\text{-}THF} c_{Ru\text{-}THF} + \varepsilon_{Ru\text{-}NEt3} c_{Ru\text{-}NEt3}} \Phi_{Ru\text{-}H} \quad (9)$$

Conclusion

Quantitative photochemical production of Ru-H^+ can be achieved via the irradiation of Ru-DMF^{2+} in a THF solution containing excess NEt_3. The chemical and quantum yields of Ru-H^+ using the system reported here were about 30 and 10^5 times higher, respectively, compared with the previously reported system. Investigations of the properties of Ru-DMF^{2+} and Ru-NEt_3^{2+} clearly indicate that the formation of Ru-H^+ proceeds via the excitation of Ru-NEt_3^{2+}, and both the higher formation and quantum yield are caused by an improvement of the photochemical ligand substitution of Ru-DMF^{2+} and thus the higher steady-state concentration of Ru-NEt_3^{2+} in THF solution.

Acknowledgment. This work was supported by a Grant-in Aid for Scientific Research on Priority Areas (417) from the Ministry of Education, Culture, Sports, Science and Technology (MEXT) of the Japanese Government.

Supporting Information Available: Full ref [2a], ^1H NMR data of $[Ru(tpy)(bpy)(CF_3SO_3)]^{2+}$ and Ru-DMF^{2+}, and Figures S1−S6. This material is available free of charge via the Internet at http://pubs.acs.org.